THE JOURNAL OF PHYSICAL CHEMISTRY A

Article

pubs.acs.org/JPCA

Deliquescence Relative Humidities of Organic and Inorganic Salts Important in the Atmosphere

Jason R. Schroeder[†] and Keith D. Beyer*

Department of Chemistry and Biochemistry, University of Wisconsin−La Crosse, La Crosse, Wisconsin 54601, United States

Supporting Information

ABSTRACT: The deliquescence relative humidities (DRH) as a function of temperature have been determined for several salts of atmospheric importance using humidity controlled thermogravimetric analysis (HTGA): sodium hydrogen oxalate monohydrate ($NaHC_2O_4·H_2O$), sodium oxalate ($Na_2C_2O_4$), sodium ammonium sulfate dihydrate ($NaNH_4SO_4·2H_2O$, lecontite), sodium hydrogen malonate monohydrate ($NaHC_3H_2O_4·H_2O$), sodium malonate monohydrate ($Na_2C_3H_2O_4·H_2O$), and ammonium hydrogen malonate ($NH_4HC_3H_2O_4$). The temperature-dependent onset DRH values (where a dry mixture begins to take up water) were also determined for mixtures of ammonium sulfate with malonic acid, and ammonium sulfate with sodium oxalates and sodium malonates, respectively. We demonstrate that the onset DRH is independent of the ratio of solids in the mixture. In general, onset DRH values were always lower than the pure component DRH values.

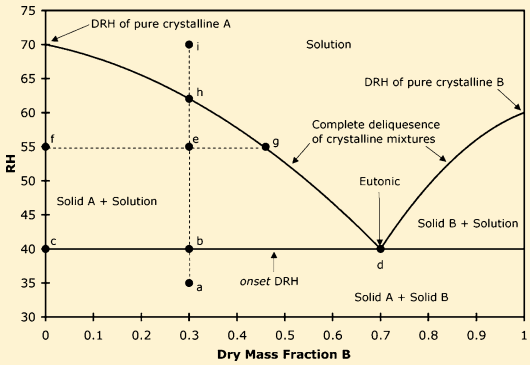

INTRODUCTION

Aerosol−cloud interactions are a major area of uncertainty in climate studies, and chemical composition is a significant driver of cloud formation and cloud phase.[1,2] Field measurements of aerosols in the free and upper troposphere (UT) have shown that the major chemical components are sulfates, nitrates, ammonium, organic species, and mineral dust.[3,4] Among the organic components, dicarboxylic acids are present in aerosols in a range of environments especially for aerosols that have undergone chemical aging.[5] Dicarboxylic acids are found in primary organic aerosols as well as secondary organic aerosols.[6] Aerosols also commonly contain mineral dust whose components can be leached to the aqueous phase through chemical aging, especially under acidic conditions.[7,8] The metals at the surface or reacted to the aqueous phase of mineral dust particles can enhance the chemistry that occurs in the aqueous phase.[7,9] Field studies have shown an abundance of aerosols with organics and metals/metal salts from sea spray (Na, Mg),[5,10−12] biomass burning (K),[13,14] and mineral dusts/meteoritic material (Na, K, Ca, Fe).[1,3,15−17] Field and lab studies have shown that metal ions can displace hydrogen ions from organic acids to form carboxylate salts in atmospheric aerosols.[10,12,18,19] For example, for a particle with dissolved NaCl and malonic acid that experienced UT temperatures and/or dry conditions, we would have

$$n\mathrm{NaCl(aq)} + \mathrm{H_2C_3H_2O_4(aq)} \rightarrow \mathrm{Na}_n\mathrm{H}_{2-n}\mathrm{C_3H_2O_4(s)} + n\mathrm{HCl(aq, g)} \quad (1)$$

where n equals one or two. Studies have shown that the HCl product is highly volatile, leaving behind the organic salt in the particle.[12,18] Recent field observations have shown that aerosols near the surface can be rapidly and efficiently transported to high altitudes in the UT via convective thunderstorms, which play a large role in the formation of cirrus clouds on synoptic and continental scales.[20−22] As the particles experience cold/dry conditions in the atmosphere, the sodium malonate salt could precipitate or contribute to glass formation of the aqueous phase of the aerosol.[19] However, there is very limited information in the literature regarding the hygroscopic properties of carboxylate salts including their effect on the hygroscopic properties of ammonium sulfate. Peng and Chan used an electrodynamic balance (EDB) to study the hygroscopic properties of particles of several sodium carboxylates at 298 K.[23] Wu et al. used a hygroscopicity tandem differential mobility analyzer (H-TDMA) to study the hygroscopic properties of several sodium oxalates with and without ammonium sulfate present at 293 K.[24] However, both of these studies reported difficulty in determining DRH values for some salts because the aerosols used in their studies could not be dried to the point of crystallization. This may be due to the limited residence time of particles under dry conditions that can be achieved in these experiments. In this study we present the temperature-dependent DRH observations for dried bulk crystals of the sodium malonates, sodium oxalates, and ammonium oxalates with and without ammonium sulfate present.

Received: August 29, 2016
Revised: November 28, 2016
Published: December 7, 2016

DOI: 10.1021/acs.jpca.6b08725
J. Phys. Chem. A 2016, 120, 9948−9957

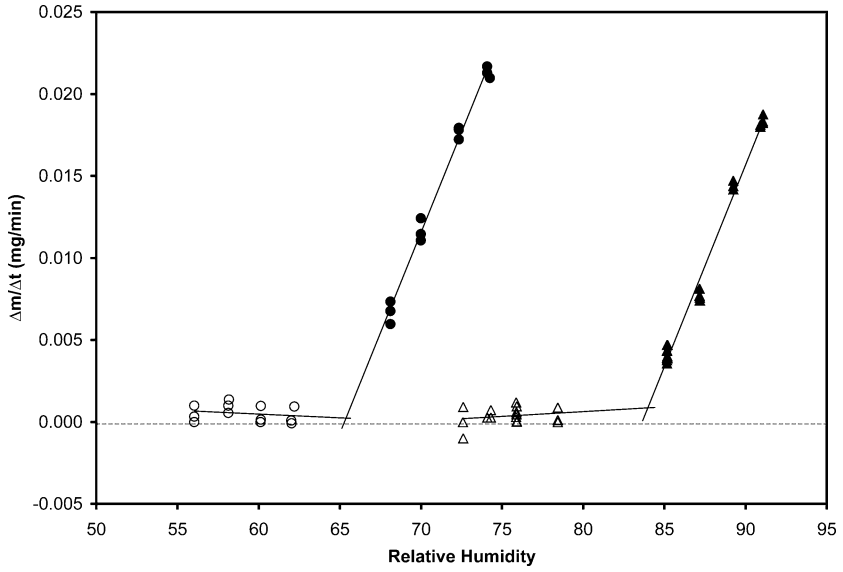

Figure 1. Plot of data from deliquescence relative humidity experiments (DRH) for $Na_2C_3H_2O_4{\cdot}H_2O$ (circles) and $NaHC_3H_2O_4{\cdot}H_2O$ (triangles). Open symbols are data before the DRH, and solid symbols are data after the DRH. In the experiments mass, temperature, heat flow, and relative humidity are simultaneously measured. Change in mass over change in time ($\Delta m/\Delta t$) is calculated for each data point and plotted vs relative humidity. Pre- and post-DRH data are then fit to respective linear equations. The intersection of these fits is the calculated DRH as shown by the intersecting lines in the plot. Dashed line marks $\Delta m/\Delta t = 0$.

EXPERIMENTAL METHODS

Sample Preparation. Dry samples for analysis were made by preparing solutions with deionized water from chemical reagents: $(NH_4)_2SO_4$, Fisher Certified ACS grade; NH_4OH, Fisher Certified ACS Plus; $H_2C_3H_2O_4$, Acros 99% ACS Reagent grade; $H_2C_2O_4{\cdot}2H_2O$, Acros 99+%; $H_2C_2O_4$, Acros 98%, anhydrous; NaOH, Fisher (beads). The concentration of all samples prepared is known to ±0.40 wt %. All solutions were made by completely dissolving solid reagents by stirring and gentle heating. The approximately 5 mL homogeneous solution was then placed in a Petri dish at room temperature and open to air for drying. Measured lab room temperature averaged 295.5 K and 64% relative humidity; however, there is significant variability about these values. Samples appeared completely dry within 24 to 48 h. The exception was $(NH_4)_2SO_4/H_2C_3H_2O_4$ mixtures where dry samples in specific mole ratios were mixed and ground together with a mortar and pestle.

The identity of the solid that precipitates from our sample solutions was confirmed by X-ray crystallography. Crystal structures were determined at the Molecular Structure Laboratory in the Chemistry Department at the University of Wisconsin−Madison. Details of how these experiments are performed can be found in the Supporting Information of Kissinger et al.[25] Briefly, a single crystal is removed from a saturated solution and placed in the instrument for analysis. The identity of the solid is determined by a match of the crystallographic data in the Cambridge Crystallographic Database (CSD). The identity of the following salts was determined with these experiments: 1:1 $NH_4OH/H_2C_2O_4$ = $NH_4HC_2O_4{\cdot}0.5H_2O$,[26] 2:1 $NH_4OH/H_2C_2O_4$ = $(NH_4)_2C_2O_4{\cdot}H_2O$,[27] and 1:1 $NH_4OH/H_2C_3H_2O_4$ = $NH_4HC_3H_2O_4$.[28]

We made $NaNH_4SO_4{\cdot}2H_2O$ (lecontite) following the method of Kloprogge et al.[29] by mixing equal moles of $(NH_4)_2SO_4$ and Na_2SO_4 in water and allowing to dry in air at room temperature. The dried crystals were placed in an ATR accessory and an infrared spectrum acquired, which is shown in Figure S1 in the Supporting Information. We found the IR spectrum was a match for lecontite as reported by Kloprogge et al.

Humidity Controlled Thermogravimetric Analysis (HTGA). The experimental apparatus and methods used to determine DRH with HTGA are described in detail in previous literature.[30] Here, we outline the main aspects of the DRH experiments. In thermogravimetric analysis (TGA) the mass of a sample is monitored to microgram accuracy as a function of temperature. With HTGA, humidified air is introduced into the sample chamber at the sample. We utilize a Mettler-Toledo TGA/DSC1 coupled to an RH-200 M humidity generator (VTI Corporation, now L&C Science and Technology.) Humidified air can be supplied in the range of 2 to 95% relative humidity (RH) at 278 to 353 K with humidity control of ±1%. RH is measured in the humidity generator with an EdgeTech dew point hygrometer, which can measure dew points in the range 233−333 K with an accuracy of ±0.2 K. To perform an experiment, a sample is placed in a 30 μL crucible made of platinum and inserted into the sample chamber along with an empty reference pan. Sample sizes were 1−15 mg with a baseline noise typically on the order of 10 μg. We did not observe any difference in DRH values as a function of sample mass for any of the pure or salt mixtures we studied. A temperature program is utilized within the software to initiate an isothermal sequence for the HTGA sample chamber. The balance temperature is maintained at 295 K by a Julabo circulator. The sample chamber temperature is controlled by a second Julabo circulator capable of achieving temperatures in the range 233−473 K, with a temperature stability of ±0.02 K. The sample temperature reading of the HTGA instrument was calibrated with an Omega Type T thermocouple (TMTSS-0326-12) connected to an Omega CSC32 readout. Both the thermocouple and readout were calibrated by Omega Engineering using instrumentation and standards traceable to the National Institute of Standards and Technology. Calibrated temperatures have an accuracy of 0.3 K.

DOI: 10.1021/acs.jpca.6b08725
J. Phys. Chem. A 2016, 120, 9948−9957

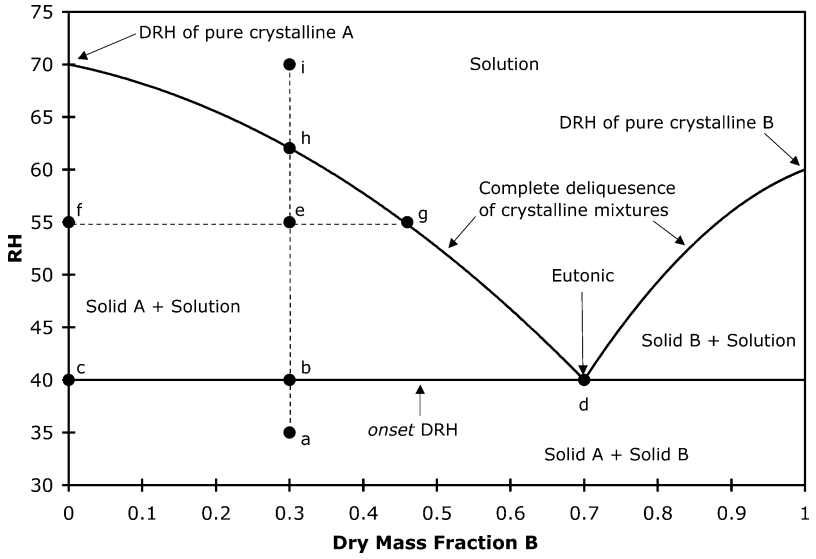

Figure 2. Theoretical dry concentration vs RH phase diagram. The various labels and regions are described in the text. Solid curves mark phase boundaries between solution, saturated solutions, and dry mixtures as labeled. Points with lower case letters are as follows: (a) dry mixture of solid A and B with a dry mass fraction of B = 0.3; (b) onset DRH, saturated solution of concentration (d) in equilibrium with solid of concentration (c); (e) saturated solution at 55% RH with concentration of (g) in equilibrium with solid of concentration (f); (h) complete DRH with solution of concentration (h); (i) solution with a dry mass fraction of B/A = 0.3 at 70% RH, no solid is present.

To determine the DRH, sample mass, heat flow, temperature, and RH are monitored simultaneously as the RH is increased stepwise. For RH values lower than the DRH, no mass change is observed (other than a small change in the mass signal as the air buoyancy changes with RH). For RH values at and higher than the DRH, the sample mass is observed to increase due to water uptake, and the rate of increase grows as the RH increases. The raw data is then plotted as RH vs $\Delta m/\Delta t$ (change in mass divided by the time interval between RH readings, 1 min in our experiments). Each data set is then fit separately to a linear equation, and these equations solved simultaneously to determine the DRH. If no water uptake was observed at 95% RH (the limit of the humidity generator), we concluded the DRH for the salt to be higher than this value. Two types of experiments were performed to establish the DRH of a compound. First a method was used covering the range 10−90% RH in 10% RH steps at the selected temperature. This experiment allows us to find the range where the DRH occurs. Then subsequent experiments are performed with RH values above and below the expected DRH. Typically, data is collected at four RH values above and below the DRH (eight RH values total). So, for example, for an expected DRH at approximately 60%, data would be collected at 52, 54, 56, 58, 62, 64, 66, and 68% RH. Each RH is maintained for 10 min during data collection or 15 min for the first RH steps pre- and post-DRH. Example plots of the data are given in Figure 1 for DRH experiments involving $NaHC_3H_2O_4{\cdot}H_2O$ and $Na_2C_3H_2O_4{\cdot}H_2O$. The same process is used to determine DRH for mixtures of compounds, such as ammonium sulfate with sodium oxalate, etc. However, in these experiments what is determined is the *onset* or *initial* DRH of the mixture.

RESULTS AND DISCUSSION

DRH for Two Compounds. For a single crystalline compound, the DRH is a single value at a specific temperature. However, when two different crystalline compounds are in contact there will be two values for the DRH at constant temperature. We illustrate this with a theoretical dry mass fraction vs RH plot in Figure 2. Here we consider two compounds with different DRH values at a given temperature. Compound A has a DRH = 70% and compound B has a DRH = 60%. Now, consider a dry mixture of these two compounds with dry mass fraction B = 0.3 at 35% RH (point a in Figure 2). When the RH is increased to 40%, point b in the figure is reached. At this point the dry mixture begins to take up water or deliquesce. This is considered the *initial* or *onset* DRH. The crystal mixture will continue to take up water at this RH until one of the compounds completely dissolves in solution (in this case compound B). When this happens equilibrium has been achieved, and the system will consist of a solution with the eutonic concentration (point d) and undissolved solute of the major compound (point c). As RH is increased the solution with undissolved A continues to take up water and the concentration of the solution follows the curve between points d and g. Note that the ratio of A to B in the system does not change, and as RH is increased to 55% (point e), the system consists of solid A of composition f in equilibrium with a solution of composition g. As RH is increased the solution composition moves along the curve from g to h and solid A continues to dissolve into solution until point h, which is the *final* or *complete* DRH of the original dry mixture. At RH above this (such as point i), no solid remains, and the ratio of compound A to B remains constant while the water content may increase or decrease as a function of RH. One can see from the diagram if a different dry mass fraction mixture were used, the onset DRH would not change. The uptake of water would begin at 40% RH until a solution of eutonic composition were formed at point d (assuming RH were held constant). Thus, the onset DRH is independent of dry mass fraction of a mixture. However, the complete DRH is clearly dependent on the initial dry mass fraction and thus will change with composition. (Also, water uptake by a particle over a range of RH is likely an indication of either a nondry particle or the presence of more than one deliquescing compounds.) The interpretation of this diagram is very similar to that of a solid/

DOI: 10.1021/acs.jpca.6b08725
J. Phys. Chem. A 2016, 120, 9948−9957

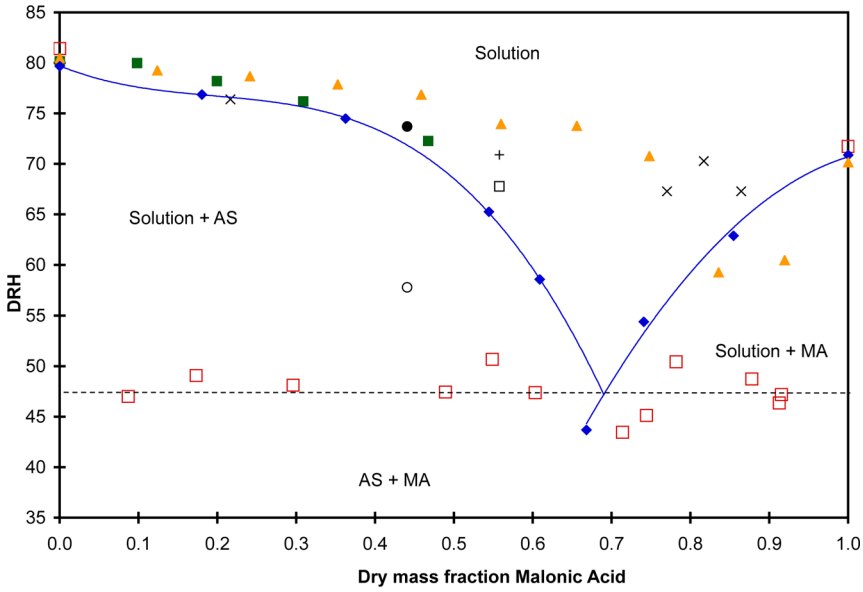

Figure 3. Dry mass fraction vs RH phase diagram for mixtures of $(NH_4)_2SO_4/H_2C_3H_2O_4$. Symbols for *onset* DRH are open red squares, results from HTGA experiments; open black circle, electrodyanamic balance experiments of Choi and Chan.[36] Symbols for *complete* DRH from RH measurements of saturated bulk solutions are black cross, Brooks et al.;[31] open black square, Wise et al.;[32] solid blue diamonds, Salcedo.[33] Symbols for *complete* DRH from video microscopy experiments are solid green squares, Parsons et al.;[34] solid orange triangles, Treuel et al.[35] Solid black circle is for complete DRH from electrodynamic balance experiments of Choi and Chan. Regions of phase stability are as labeled in the diagram. Blue curves connecting the points of Salcedo are fits to the data as described in the text. Dashed line is the average of the HTGA data: 47.5 ± 1.9% RH.

liquid phase diagram where composition and temperature are the axes, and the lever rule can similarly be used to determine the amount of substance in each phase. However, the experimental determination of a dry composition vs RH phase diagram is much more challenging than a similar composition vs temperature solid/liquid phase diagram. From this example, we also see that the onset DRH is an important atmospheric value, as it is the point at which dry particles will begin to take up water and form a solution. The complete DRH, where all solid has dissolved, will be at a higher RH dependent on the dry mass fraction of the mixture. However, at the eutonic concentration and for a single compound the onset DRH is equal to the complete DRH. Several different experiments are able to measure the complete DRH (discussed below); however, there are few experiments that have measured the onset DRH.

Ammonium Sulfate/Malonic Acid. In our experiments, we are able to measure the *onset* DRH. As a test case, we measured the onset DRH for dry mixtures of ammonium sulfate and malonic acid, a system for which there is literature DRH data. Brooks et al.,[31] Wise et al.,[32] and Salcedo[33] determined the complete DRH by measuring the RH or water vapor pressure over saturated solutions. Parsons et al.[34] and Treuel et al.[35] determined the complete DRH using video microscopy of particles deposited on slides, and Choi and Chan[36] determined complete DRH from the growth of particles in an electrodynamic balance. The results of these studies are all plotted in Figure 3 along with our results for the onset DRH in this system with the raw data listed in Table S1 in the Supporting Information. Only Choi and Chan determined both the onset DRH and the complete DRH in this system, though only for one concentration: 1:1 dry mole ratio of $(NH_4)_2SO_4/H_2C_3H_2O_4$. Several features are seen in Figure 3. First, there is good agreement for the DRH of pure $(NH_4)_2SO_4$ and $H_2C_3H_2O_4$ using very different techniques. There is also reasonable agreement among the different techniques for complete DRH at low dry mass fraction of malonic acid. However, disagreement becomes significant at dry mass fractions of malonic acid greater than about 0.4, where differences in complete DRH are as large as 30% RH. With respect to the onset DRH, there is some scatter in the onset DRH from our HTGA measurements with an average value of 47.5 ± 1.9% RH, though not outside the accuracy of our RH measurements.[37] In contrast, Choi and Chan report an onset DRH of 57.8%. These onset DRH values should also correlate with the lowest complete DRH, which would occur at the eutonic composition (theoretical point d in Figure 2). In the data of Treuel et al. this occurs at 0.84 dry mass fraction malonic acid and 59.3% RH. This is in good agreement with the onset DRH value of Choi and Chan, but much higher than our value from HTGA experiments. In general the complete DRH values of Treuel et al. are higher than those of Salcedo in the region of 0.5 to 0.8 dry mass fraction malonic acid, so this result is not surprising.

The lowest complete DRH value of Salcedo is at 0.67 dry mass fraction malonic acid and 43.7% RH. This is much closer to our value for the onset DRH of 47.5%, but still outside the uncertainty in our onset DRH value. In Salcedo's experiments she started with a solution that was unsaturated in both salts. The RH was measured above this solution and then the concentration of one solute was increased, while the concentration of the other solute was held constant, and the RH measured after each addition of solute. In this method, it is possible to supersaturate the solution with respect to the solute held constant. If the point at 43.7% RH is a eutonic point, then it represents equilibrium between both series of DRH points, which constitute solubility curves for malonic acid and ammonium sulfate, respectively. Salcedo determined that polynomial equations were equally accurate at fitting her data as the AIM III or UNIFAC models (see her Figure 1). Thus, we also use polynomial fits to her saturation data for our analysis. When the data point at 43.7% RH is included in the solubility

DOI: 10.1021/acs.jpca.6b08725
J. Phys. Chem. A 2016, 120, 9948−9957

curve for malonic acid in this system (right side of Figures 3 and S2 in the Supporting Information), the data can reasonably be fit to a second order polynomial (Figure S2). However, including this point with the DRH data along the ammonium sulfate solubility curve (left side of Figures 3 and S2) leads to a poor fit for second or third order polynomial equations. Without this data point the DRH data constituting an ammonium sulfate solubility curve is reasonably fit to a second order polynomial, and an excellent fit to a third order polynomial, which is the fit we present in Figures 3 and S2. This analysis leads to the possibility of Salcedo's DRH value at 43.7% being a state of supersaturation with respect to ammonium sulfate.

Salcedo did not state which solute was added and which was held constant in her experiments; however, we plotted the dry mass fraction of malonic acid vs RH in the mixtures she studied (see the Supporting Information to her paper) in our Figure S2. For the series of experiments where the lowest DRH was measured, the concentration of ammonium sulfate was held constant while increasing malonic acid (constant 28 wt % ammonium sulfate as seen in Figure 1 of Salcedo). We have connected the concentration of samples in this series with a red curve in Figure S2. In this interpretation, it is seen that the concentration of the series crosses the ammonium sulfate solubility curve and terminates at the "DRH" Salcedo determined at 43.7% RH, which lies on the malonic acid solubility curve. As mentioned above, this series of observations is possible where one solute (malonic acid) is added to a solution that contains a second dissolved solute (ammonium sulfate). The added solute dissolves until it reaches its saturation point in the solution; however, the second, dissolved solute may supersaturate as its concentration changes without overcoming the nucleation barrier to precipitate from solution. We believe this is a plausible explanation for the results of Salcedo with respect to the lowest DRH data point. It is then seen in Figure 3 that the intersection of the two fitted solubility curves connecting the DRH values of Salcedo falls directly in line with the average of our onset DRH value. The calculated eutonic from the equations fit to Salcedo's data is 47.2% RH at a malonic acid dry mass fraction of 0.690, which is in excellent agreement with our average onset DRH value of 45.7% RH.

It is unclear why there are such large differences in the complete DRH values at moderate to high dry mass fraction malonic acid in this system from various groups and techniques. Were solids other than $(NH_4)_2SO_4$ or $H_2C_3H_2O_4$ forming in solution, the DRH could be affected. However, Beyer et al.[37] studied solubility in the $(NH_4)_2SO_4/H_2C_3H_2O_4/H_2O$ system, and found no evidence (from infrared spectroscopy experiments) that other solids were forming at room temperature. Thus, we observe that our interpretation of the data of Salcedo for complete DRH combined with our HTGA results for onset DRH most closely match the theoretical DRH behavior for a two compound mixture as illustrated in Figure 2.

$NaHC_2O_4$ with and without $(NH_4)_2SO_4$. DRH experiments as a function of temperature were performed for sodium hydrogen oxalate monohydrate ($NaHC_2O_4{\cdot}H_2O$, the solid that forms at room temperature from an aqueous solution that is 1:1 $NaOH/H_2C_2O_4$[38]) both with and without ammonium sulfate present. The DRH for $NaHC_2O_4{\cdot}H_2O$ was determined to be greater than 95% for 298 and 308 K (and by implication 288 K since DRH increases with decreasing temperature), which is the RH limit of our experimental technique. The average DRH values for the pure salts we studied are given in Table 2. We then determined the onset DRH of solids completely dried from mixtures of $NaHC_2O_4$ and $(NH_4)_2SO_4$. Buttke et al.[38] determined that the ratio of $(NH_4)_2SO_4/NaHC_2O_4$ in saturated solution determines which solids form. For high $(NH_4)_2SO_4/NaHC_2O_4$ ratio, ammonium hydrogen oxalate hemihydrate ($NH_4HC_2O_4{\cdot}0.5H_2O$) is the least soluble solid at room temperature, while at low $(NH_4)_2SO_4/NaHC_2O_4$ ratio, $NaHC_2O_4{\cdot}H_2O$ is the least soluble solid at room temperature (see summary in Table 1). Thus, we made samples at both low and high $(NH_4)_2SO_4/NaHC_2O_4$ ratios: 1.2 and 5.7, respectively for onset DRH experiments. At low $(NH_4)_2SO_4/NaHC_2O_4$ ratios, the solids present in a completely dry mixture should be simply $NaHC_2O_4{\cdot}H_2O$ and $(NH_4)_2SO_4$. Thus, the temperature-dependent onset DRH we measured is for a mixture of these two solids. The results are given in Figure 4, and the raw data is given in Table S2 in the Supporting Information. Average DRH values for the salt mixtures we studied are given in Table 3. In Figure 4 we see the onset DRH of the mixture is lower than that of ammonium sulfate, as expected, and there is slightly higher temperature dependence to the onset DRH than observed for ammonium sulfate.

Table 1. Summary of Solids Predicted to Be Present in Completely Effloresced Samples as a Function of the Composition of the Mother Solution for Aqueous Solutions of $(NH_4)_2SO_4$ and Sodium Oxalates

$[(NH_4)_2SO_4]$ (wt %)	[organic salt] (wt %)	$(NH_4)_2SO_4$/oxalate salt mol ratio	solids
		$NaHC_2O_4$	
10	7	1.2	$NaHC_2O_4{\cdot}H_2O$ + $(NH_4)_2SO_4$
20	3	5.7	$NH_4HC_2O_4{\cdot}0.5H_2O$/ $(NH_4)_2SO_4/Na_2SO_4{\cdot}10H_2O$ OR $NH_4HC_2O_4{\cdot}0.5H_2O$/ $NaNH_4SO_4{\cdot}2H_2O/(NH_4)_2SO_4$
		$Na_2C_2O_4$	
5	5.9	0.86	$Na_2C_2O_4$ + $(NH_4)_2SO_4$
20	6	3.4	$(NH_4)_2C_2O_4{\cdot}H_2O/(NH_4)_2SO_4/$
10	2	5.1	$Na_2SO_4{\cdot}10H_2O$ OR $(NH_4)_2C_2O_4{\cdot}H_2O/NaNH_4SO_4{\cdot}$ $2H_2O/(NH_4)_2SO_4$

At high $(NH_4)_2SO_4/NaHC_2O_4$ ratios, $NH_4HC_2O_4{\cdot}0.5H_2O$ is the least soluble solid.[38] Ammonium and sulfate ions are in large excess in the solution such that upon further drying $(NH_4)_2SO_4$ will likely be one of the precipitates. However, one or two solids can form with the sodium ions that remain: $NaNH_4SO_4{\cdot}2H_2O$ (lecontite) and/or $NaSO_4{\cdot}10H_2O$. Differential scanning calorimetry (DSC) experiments performed by Buttke et al.[38] showed that the sulfate-containing solid(s) dissolves at the ternary eutectic; thus, it is not possible to separate the solid for analysis from solution. Therefore, our results for high $(NH_4)_2SO_4$:$NaHC_2O_4$ ratio represent the onset DRH for a mixture of $NH_4HC_2O_4{\cdot}0.5H_2O$, $(NH_4)_2SO_4$, $Na_2SO_4{\cdot}10H_2O$ or a mixture of $NH_4HC_2O_4{\cdot}0.5H_2O$, $NaNH_4SO_4{\cdot}2H_2O$, $(NH_4)_2SO_4$ (listed in the order each salt could precipitate from solution). Temperature-dependent DRH values for $Na_2SO_4{\cdot}10H_2O$ are known,[39] but those for $NH_4HC_2O_4{\cdot}0.5H_2O$ or $NaNH_4SO_4{\cdot}2H_2O$ have not been previously published to our knowledge. In our experiments we determined that dry crystals of $NH_4HC_2O_4{\cdot}0.5H_2O$ did not take up water at 95% RH at 298 or 308 K; thus, the DRH > 95%. Crystals of lecontite were used for DRH experiments as a function of temperature, and the results are given in Figure 4

DOI: 10.1021/acs.jpca.6b08725
J. Phys. Chem. A 2016, 120, 9948−9957

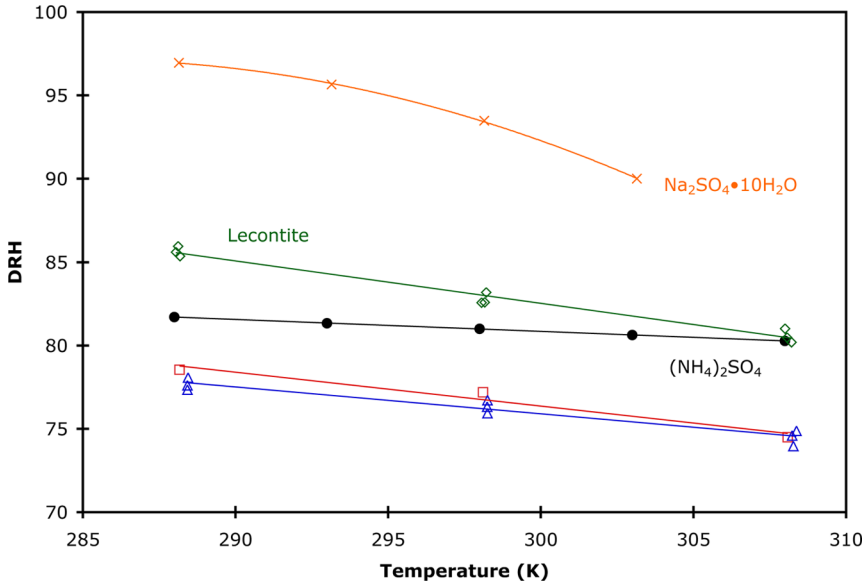

Figure 4. DRH as a function of temperature for several salts as described in the text involving or for comparison to $NaHC_2O_4{\cdot}H_2O$. Symbols for the DRH of pure salts are as labeled in the figure. Salt mixtures are (red squares) solids dried from a mixture with a $(NH_4)_2SO_4/NaHC_2O_4$ mole ratio = 5.7 and (blue triangles) solids dried from a mixture with a $(NH_4)_2SO_4/NaHC_2O_4$ mole ratio = 1.2.

(raw data is given in Table S3 in the Supporting Information with average values listed in Table 2) along with the literature data for $Na_2SO_4{\cdot}10H_2O$ and the onset DRH data for the $NH_4HC_2O_4{\cdot}0.5H_2O/(NH_4)_2SO_4$/lecontite and/or $Na_2SO_4{\cdot}10H_2O$ dry mixture. The onset DRH values for this mixture are nearly coincident with those of the $NaHC_2O_4{\cdot}H_2O/(NH_4)_2SO_4$ mixture. Therefore, even though the ammonia content affects whether $NaHC_2O_4{\cdot}H_2O$ or $NH_4HC_2O_4{\cdot}0.5H_2O$ forms from solution, the onset DRH values for dry mixtures of these solids with ammonium and sodium sulfate salts are not affected. This is likely because the sulfate salts dominate the DRH values since they are present in much larger amounts than the oxalate salts. Also, we note that the DRH of both $NaHC_2O_4{\cdot}H_2O$ and $NH_4HC_2O_4{\cdot}0.5H_2O$ is >95% at the temperatures we studied. Thus, we conclude they will have the same effect on the onset DRH of a mixture involving either salt, as seen in our results. Even though the mixture with

Table 2. Average DRH of Each Pure Salt as a Function of Temperature from Our Experiments

temperature (K)	288	298	308
$NaHC_2O_4{\cdot}H_2O$	>95	>95	>95
$NH_4HC_2O_4{\cdot}0.5H_2O$	>95	>95	>95
$Na_2C_2O_4$	75.4	75.3	75.6
$(NH_4)_2C_2O_4{\cdot}H_2O$	>95	>95	>95
$NaHC_3H_2O_4{\cdot}H_2O$	87.0	84.8	81.9
$Na_2C_3H_2O_4{\cdot}H_2O$	66.5	65.3	64.7
$NH_4HC_3H_2O_4$	74.3	69.1	66.5
$NaNH_4SO_4{\cdot}2H_2O$	85.6	82.8	80.6

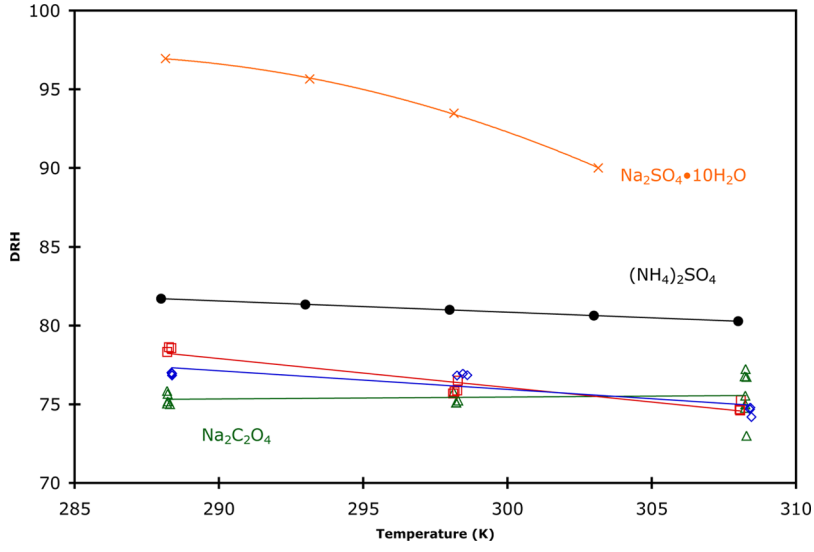

Figure 5. DRH as a function of temperature for several salts as described in the text involving or for comparison to $Na_2C_2O_4$. Symbols for the DRH of pure salts are as labeled in the figure. Salt mixtures are (red squares) solids dried from a mixture with a $(NH_4)_2SO_4/Na_2C_2O_4$ mole ratio = 5.1 or 3.4 and (blue triangles) solids dried from a mixture with a $(NH_4)_2SO_4/Na_2C_2O_4$ mole ratio = 0.86.

DOI: 10.1021/acs.jpca.6b08725
J. Phys. Chem. A 2016, 120, 9948−9957

$NH_4HC_2O_4 \cdot 0.5H_2O$ will have other sulfate salts present (lecontite and/or $Na_2SO_4 \cdot 10H_2O$), these salts are present in much smaller quantities than ammonium sulfate and thus likely have a very minor influence on the onset DRH.

$Na_2C_2O_4$ with and without $(NH_4)_2SO_4$. DRH experiments as a function of temperature were performed for sodium oxalate ($Na_2C_2O_4$, the solid that forms at room temperature from a solution that is 2:1 $NaOH/H_2C_2O_4$[38]) both with and without ammonium sulfate present. It was found that the DRH for $Na_2C_2O_4$ varied little with temperature (average values as a function of temperature are listed in Table 2), and values are plotted as red squares in Figure 5 with raw data given in Table S4 in the Supporting Information. Given that the DRH values for $NaHC_2O_4 \cdot H_2O$ are >95% while those of $Na_2C_2O_4$ are ∼75%, we see there is a dramatic difference in the DRH dependent on whether the sodium/oxalate ratio is 1:1 vs 2:1. This implies a significant difference in the crystal structures where $Na_2C_2O_4$ is able to accommodate water molecules more readily than $NaHC_2O_4 \cdot H_2O$. There is likely additional water affinity in $Na_2C_2O_4$ due to the additional sodium ion in the unit cell.

We also determined the onset DRH for $Na_2C_2O_4/(NH_4)_2SO_4$ mixtures. Buttke et al.[38] determined that the ratio of $(NH_4)_2SO_4/Na_2C_2O_4$ in saturated solutions determines which solids form; however, they determined that only at the lowest $(NH_4)_2SO_4/Na_2C_2O_4$ ratios (<1) did $Na_2C_2O_4$ form as the least soluble solid (see Table 1 for a summary). For higher ratios, the least soluble solid was $(NH_4)_2C_2O_4 \cdot H_2O$. With this solid removed from solution, Na^+, NH_4^+, and SO_4^{2-} ions remain. Which solids form from solution will depend on the next least soluble solid. If ammonium sulfate precipitates first, the remaining ions are Na^+ and SO_4^{2-} in a 2:1 ratio. Thus, $Na_2SO_4 \cdot 10H_2O$ is the third salt that could form. The reverse is also true, if $Na_2SO_4 \cdot 10H_2O$ forms second, then the remaining ions (2:1 NH_4^+:SO_4^{2-}) can form $(NH_4)_2SO_4$. However, if $NaNH_4SO_4 \cdot 2H_2O$ were the least soluble solid after $(NH_4)_2C_2O_4 \cdot H_2O$, then the ions that remain would be NH_4^+ and SO_4^{2-} in a 2:1 ratio. Thus, $(NH_4)_2SO_4$ is the third salt that can form in this scenario. Both of these scenarios would be possible for both of the $(NH_4)_2SO_4/Na_2C_2O_4$ ratios we studied (3.4 and 5.1). These two possible combinations of precipitating salts are summarized in Table 1. We were not able to determine which solids precipitated upon further drying of our solutions. However, our onset DRH values are likely for $(NH_4)_2C_2O_4 \cdot H_2O$ with some combination of $(NH_4)_2SO_4/Na_2SO_4 \cdot 10H_2O$ or $NaNH_4SO_4 \cdot 2H_2O/(NH_4)_2SO_4$. Temperature-dependent DRH values for $(NH_4)_2C_2O_4 \cdot H_2O$ have not been previously published to our knowledge. In our experiments we found that dry $(NH_4)_2C_2O_4 \cdot H_2O$ crystals did not take up water at 95% RH at 298 or 308 K; thus, the DRH > 95%. We made two solutions with high $(NH_4)_2SO_4/Na_2C_2O_4$ ratios as given in Table 1 and performed DRH experiments on the crystals that remained after completely drying these solutions. All data points are plotted in Figure 5 with raw data given in Table S5 in the Supporting Information and average values listed in Table 3. No difference was observed in the onset DRH values as a function of which ratio was used. This is in agreement with our results described earlier for the $(NH_4)_2SO_4/H_2C_3H_2O_4$ system and theory that the onset DRH is independent of the ratio of crystals in mixtures with the same solids present.

We also made one solution with a low $(NH_4)_2SO_4/Na_2C_2O_4$ ratio as given in Table 1. The least soluble solid in this mixture is expected to be $Na_2C_2O_4$, and thus, the other crystal that precipitates upon complete drying should be $(NH_4)_2SO_4$. We performed DRH experiments on this dry mixture as a function of temperature with the results given in Figure 5, raw data given in Table S5 in the Supporting Information, and average values listed in Table 3. It is seen that the measured onset DRH values are very similar to those of the dry mixtures at high $(NH_4)_2SO_4$:$Na_2C_2O_4$ ratios. Thus, again (as in the case of the $(NH_4)_2SO_4/NaHC_2O_4$ mixtures), we observe that there is little change in onset DRH when ammonium vs sodium oxalate solids precipitate in this system.

Table 3. Average DRH of Dry Mixtures of $(NH_4)_2SO_4$ with Organic Salt as a Function of Temperature from Our Experiments

	$(NH_4)_2SO_4$/oxalate salt mol ratio	temperature (K)		
		288	298	308
$NaHC_2O_4/(NH_4)_2SO_4$	5.7	78.5	77.2	74.5
	1.2	77.7	76.3	74.5
$Na_2C_2O_4/(NH_4)_2SO_4$	3.4 or 5.1	74.9	76.0	78.5
	0.86	74.6	76.9	76.9
$NaHC_3H_2O_4/(NH_4)_2SO_4$	0.76	69.7	63.4	56.8
$Na_2C_2O_4/(NH_4)_2SO_4$	1.1 or 1.7	crystals could not be dried		

Sodium Salts of Malonic Acid. DRH experiments as a function of temperature were performed for sodium hydrogen malonate monohydrate ($NaHC_3H_2O_4 \cdot H_2O$, the solid that forms at room temperature from an aqueous solution that is 1:1 $NaOH/H_2C_3H_2O_4$[25]) and sodium malonate monohydrate ($Na_2C_3H_2O_4 \cdot H_2O$, the solid that forms at room temperature from a solution that is 2:1 $NaOH/H_2C_3H_2O_4$[25]). Typical results of DRH experiments for both solids at 298 K are given in Figure 1. A plot of DRH as a function of temperature for $NaHC_3H_2O_4 \cdot H_2O$ and $Na_2C_3H_2O_4 \cdot H_2O$ is given in Figure 6 (open symbols) along with data for malonic acid[40] for comparison. Raw data is given in Table S6 in the Supporting Information with average values reported in Table 2. We observe that $NaHC_3H_2O_4 \cdot H_2O$ has the highest DRH followed by $H_2C_3H_2O_4$ and then $Na_2C_3H_2O_4 \cdot H_2O$ with the lowest DRH. The activity of water in a solution is equal to the RH expressed as a fraction. For an ideal solution the activity is equal to the mole fraction, thus the lower the water content of an ideal solution, the lower the DRH. Deviations from this relationship can indicate the level of nonideality of a solution:

$$a_i = \gamma_i x_i \quad (2)$$

where a_i is the activity of component i, x_i is the mole fraction of component i, and γ_i is the activity coefficient of component i. Thus, for an ideal solution the activity coefficient is unity, and for real solutions it will be a different value. Now, we can contrast the DRH values with the solubility of each salt over the same temperature range. We have plotted the temperature-dependent solubility of each salt as the mole fraction of water present at saturation (solid symbols in Figure 6) for malonic acid,[41] $NaHC_3H_2O_4 \cdot H_2O$, and $Na_2C_3H_2O_4 \cdot H_2O$.[25] First, we notice that for each compound the mole fraction of water present is higher than the DRH (thus activity value) at all temperatures. Therefore, we can immediately state that the activity coefficient for each salt is less than one over the temperature range studied, and thus the water−solute interactions are more favorable than the water−water or

DOI: 10.1021/acs.jpca.6b08725
J. Phys. Chem. A 2016, 120, 9948−9957

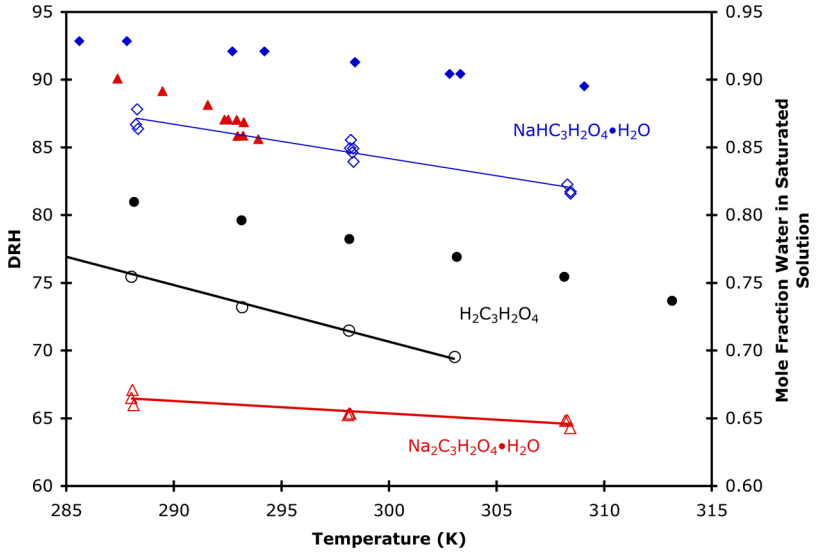

Figure 6. DRH (open symbols with scale on left) as a function of temperature for the following: (blue) $NaHC_3H_2O_4 \cdot H_2O$, (black) $H_2C_3H_2O_4$ from Beyer et al.,[40] (red) $Na_2C_3H_2O_4 \cdot H_2O$. Solute solubilities represented by mole fraction of water in a saturated solution (solid symbols with scale on right) as a function of temperature: (blue) $NaHC_3H_2O_4 \cdot H_2O$ from Kissinger et al.,[25] (black) malonic acid from Apleblat and Manzurola,[41] (red) $Na_2C_3H_2O_4 \cdot H_2O$ from Kissinger et al.[25] Lines are fits to the DRH data.

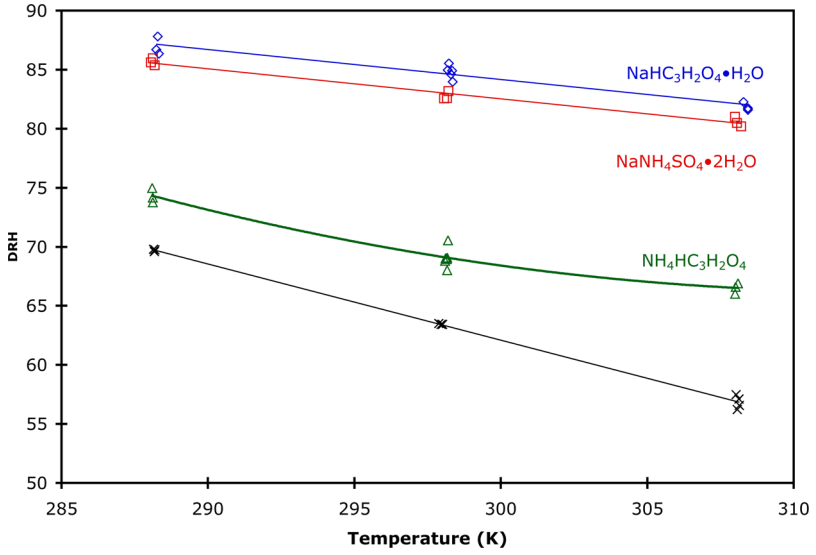

Figure 7. DRH as a function of temperature for the following: (blue) $NaHC_3H_2O_4 \cdot H_2O$, (red) $NaNH_4C_3H_2O_4$, (green) $NH_4HC_3H_2O_4$, (black) onset DRH for solids dried from a mixture with a $(NH_4)_2SO_4/NaHC_3H_2O_4$ mole ratio = 0.76.

solute−solute interactions for each solution. We take particular note that for $Na_2C_3H_2O_4 \cdot H_2O$, the solute−water interactions must be particularly strong as the DRH is far lower (thus water activity) than what would be expected from the very high mole fraction of water present at saturation. For example, at 288 K we see DRH = 66%, and thus, the water activity is 0.66; however, the water mole fraction at this temperature at saturation is 0.90 leading to a γ for water of 0.73. In contrast water activity coefficients for malonic acid and $NaHC_3H_2O_4$ solutions are greater than 0.9. Possibly the low water activity coefficients in $Na_2C_3H_2O_4$ solutions are not surprising since there must be very strong interactions between water and the two sodium ions present for each solute molecule. As the number of sodium ions decreases ($NaHC_3H_2O_4$ and $H_2C_3H_2O_4$), these interactions would be significantly weakened.

We also measured the onset DRH of the crystals resulting from a completely dried mixture of 20/25% $(NH_4)_2SO_4/NaHC_3H_2O_4$ solution, which has a dry mole ratio $(NH_4)_2SO_4/NaHC_3H_2O_4$ of 0.76. Kissinger et al.[25] determined that these crystals are a mixture of lecontite ($NaNH_4SO_4 \cdot 2H_2O$) and $NaHC_3H_2O_4 \cdot H_2O$. They also determined $Na_2SO_4 \cdot 10H_2O$ is the least soluble solid at low mole ratio $(NH_4)_2SO_4/NaHC_3H_2O_4$ (0.32), while ammonium sulfate is the least soluble solid at high mole ratio $(NH_4)_2SO_4/NaHC_3H_2O_4$ (2.95). Thus, which solids are present in a completely dry sample will depend on the dry mole ratio. However, we focused on the midrange of ratios of $(NH_4)_2SO_4/NaHC_3H_2O_4$ where lecontite is the least soluble solid. With a dry mole ratio $(NH_4)_2SO_4/NaHC_3H_2O_4$ of 0.76, the bisulfate ion is limiting in our mixtures, and thus, all of the sulfate would be consumed producing lecontite along with some of the sodium and ammonium ions. Once $NaHC_3H_2O_4 \cdot H_2O$ has also precipitated

DOI: 10.1021/acs.jpca.6b08725
J. Phys. Chem. A 2016, 120, 9948−9957

(consuming the remaining sodium ions) there will be an excess of ammonium and hydrogen malonate ions. Upon complete drying the solid that likely forms from the remaining ions is $NH_4HC_3H_2O_4$. Thus, we conclude the onset DRH values we report are for the dry mixture: $NaNH_4SO_4{\cdot}2H_2O$/$NH_4HC_3H_2O_4$/$NaHC_3H_2O_4{\cdot}H_2O$ in a 1:0.75:0.25 mol ratio, respectively, and the results are given in Figure 7 (with raw data given in Table S8 in the Supporting Information and average values listed in Table 3) where a very strong temperature dependence is seen. With respect to $NH_4HC_3H_2O_4$, Braban reported that no crystallization occurred in bulk solutions or in aerosol efflorescence experiments even after most of the solution volume had been evaporated.[42] However, we were able to grow crystals of $NH_4HC_3H_2O_4$ from a 1:1 NH_4OH:$H_2C_3H_2O_4$ aqueous solution. These crystals were air-dried at room temperature for 1 week, and then the DRH measured as a function of temperature. Values are given in Figure 7. If we compare the DRH of the various samples, the onset DRH of the dry mixture $NaNH_4SO_4{\cdot}2H_2O$/$NH_4HC_3H_2O_4$/$NaHC_3H_2O_4{\cdot}H_2O$ is lower than the DRH of pure $NaNH_4SO_4{\cdot}2H_2O$, $NaHC_3H_2O_4{\cdot}H_2O$, or $NH_4HC_3H_2O_4$, as expected. Among these pure compounds, $NaHC_3H_2O_4{\cdot}H_2O$ and lecontite have the highest DRH values, and their temperature dependencies mirror each other. $NH_4HC_3H_2O_4$ has much lower DRH values and is likely the major influence on the significant lowering of the onset DRH of the three compound mixture. If we compare the temperature-dependent DRH values with each salt's corresponding solubility, the expected correlation is observed: more soluble salts have lower DRH values. However, a shortcoming to this comparison is we do not have solubility data for the mixture ($NaNH_4SO_4{\cdot}2H_2O$/$NH_4HC_3H_2O_4$/$NaHC_3H_2O_4{\cdot}H_2O$) or lecontite. Lecontite does not have a solubility equilibrium in water without other species present.[25]

We also attempted to measure the DRH of crystals from dried $(NH_4)_2SO_4$/$Na_2C_3H_2O_4$ solutions with concentrations 30/20 and 20/20 wt % $(NH_4)_2SO_4$/$Na_2C_3H_2O_4$. The first solution was dried in a vacuum oven at 323 K for several days, and the latter solution was air-dried at room temperature for 2 weeks, and then dried in a vacuum oven at 323 K for several days. We occasionally ran DRH experiments during the drying period on both samples. In both cases a clear DRH was never observed, but rather a smooth increase in water uptake as a function of relative humidity. From this we conclude that our $(NH_4)_2SO_4$/$NaHC_3H_2O_4$ samples were never completely dry, and the mixture of solids present is quite hydrophilic.

CONCLUSIONS

We measured the DRH of several pure solids over the range 288−308 K: $NaHC_2O_4{\cdot}H_2O$, $NH_4HC_2O_4{\cdot}0.5H_2O$, $Na_2C_2O_4$, $(NH_4)_2C_2O_4{\cdot}H_2O$, $NaHC_3H_2O_4{\cdot}H_2O$, $Na_2C_3H_2O_4{\cdot}H_2O$, $NH_4HC_3H_2O_4$, and $NaNH_4SO_4{\cdot}2H_2O$ (lecontite). For $NaHC_2O_4{\cdot}H_2O$, $NH_4HC_2O_4{\cdot}0.5H_2O$, and $(NH_4)_2C_2O_4{\cdot}H_2O$ the DRH was found to be >95% at 298 and 308 K, while for $Na_2C_2O_4$ it was found to be relatively constant with temperature at 75.5%. For $NaHC_3H_2O_4{\cdot}H_2O$ and $Na_2C_3H_2O_4{\cdot}H_2O$, the latter had much lower DRH than the former even though their solubilities in water are similar. Thus, for the sodium malonates, the number of sodium ions present has a strong impact on DRH values for the pure salts.

We measured the onset DRH for dry mixtures of malonic acid and ammonium sulfate for comparison with literature data. We found reasonable agreement between our onset DRH values and the lowest complete DRH value reported by Salcedo. We further demonstrated that the onset DRH is independent of the ratio of solids in a dry mixture. We also measured the onset DRH as a function of temperature of dry mixtures of ammonium sulfate with sodium oxalates and malonates, respectively. Kissinger et al.[25] and Buttke et al.[38] determined that the solids present in these mixtures depends on the $(NH_4)_2SO_4$/sodium oxalates and $(NH_4)_2SO_4$/sodium malonates ratios, respectively. In the case of the $(NH_4)_2SO_4$/sodium oxalates mixtures, we found the different ratios did not affect the onset DRH of the mixtures even though it was likely different solids were present. However, while we were able to measure DRH values for mixtures of $(NH)_4SO_4$/$NaHC_3H_2O_4$, we were unable to completely dry bulk mixtures of $(NH)_4SO_4$/$Na_2C_3H_2O_4$, thus indicating very different hygroscopic properties. In all cases the onset DRH values for mixtures were lower than the DRH values of the salts that composed the mixtures.

ASSOCIATED CONTENT

Supporting Information

The Supporting Information is available free of charge on the ACS Publications website at DOI: 10.1021/acs.jpca.6b08725.

All raw DRH data from our HTGA experiments; IR spectrum for a dry sample that is 1:1 $(NH_4)_2SO_4$/Na_2SO_4; plot and analysis of the data of Salcedo[33] (PDF)

AUTHOR INFORMATION

Corresponding Author

*E-mail: kbeyer@uwlax.edu.

ORCID

Keith D. Beyer: 0000-0003-0630-7575

Present Address

†Currently at NASA postdoctoral program, NASA Langley Research Center, Hampton, Virginia, USA.

Notes

The authors declare no competing financial interest.

ACKNOWLEDGMENTS

We wish to thank Anastasiya Vinokur and Dr. Ilia Guzei at the University of Wisconsin−Madison for running and analyzing the X-ray crystallography experiments, Lukas Buttke for performing some of the HTGA experiments, and anonymous reviewers for helpful comments on our manuscript. This work was supported by the NSF Atmospheric Chemistry Program (AGS-1361592).

REFERENCES

(1) Cziczo, D. J.; Froyd, K. D.; Hoose, C.; Jensen, E. J.; Diao, M.; Zondlo, M. A.; Smith, J. B.; Twohy, C. H.; Murphy, D. M. Clarifying the Dominant Sources and Mechanisms of Cirrus Cloud Formation. *Science* **2013**, *340* (6138), 1320−1324.

(2) DeMott, P. J.; Prenni, A. J.; Liu, X.; Kreidenweis, S. M.; Petters, M. D.; Twohy, C. H.; Richardson, M. S.; Eidhammer, T.; Rogers, D. C. Predicting Global Atmospheric Ice Nuclei Distributions and Their Impacts on Climate. *Proc. Natl. Acad. Sci. U. S. A.* **2010**, *107* (25), 11217−11222.

(3) Murphy, D. M.; Thomson, D. S.; Mahoney, T. M. J. In Situ Measurements of Organics, Meteoritic Material, Mercury, and Other Elements in Aerosols at 5 to 19 Kilometers. *Science* **1998**, *282*, 1664−1669.

(4) Froyd, K. D.; Murphy, D. M.; Lawson, P.; Baumgardner, D.; Herman, R. L. Aerosols That Form Subvisible Cirrus at the Tropical Tropopause. *Atmos. Chem. Phys.* **2010**, *10* (1), 209−218.

DOI: 10.1021/acs.jpca.6b08725
J. Phys. Chem. A 2016, 120, 9948−9957

(5) Sullivan, R. C.; Prather, K. A. Investigations of the Diurnal Cycle and Mixing State of Oxalic Acid in Individual Particles in Asian Aerosol Outflow. *Environ. Sci. Technol.* **2007**, *41* (23), 8062−8069.
(6) Seinfeld, J. H.; Pandis, S. N. *Atmospheric Chemistry and Physics: From Air Pollution to Climate Change*; Wiley: New York, 1998.
(7) Harris, E.; Sinha, B.; Foley, S.; Crowley, J. N.; Borrmann, S.; Hoppe, P. Sulfur Isotope Fractionation during Heterogeneous Oxidation of SO2 on Mineral Dust. *Atmos. Chem. Phys.* **2012**, *12* (11), 4867−4884.
(8) Reitz, P.; Spindler, C.; Mentel, T. F.; Poulain, L.; Wex, H.; Mildenberger, K.; Niedermeier, D.; Hartmann, S.; Clauss, T.; Stratmann, F.; Sullivan, R. C.; DeMott, P. J.; Petters, M. D.; Sierau, B.; Schneider, J. Surface Modification of Mineral Dust Particles by Sulphuric Acid Processing: Implications for Ice Nucleation Abilities. *Atmos. Chem. Phys.* **2011**, *11* (15), 7839−7858.
(9) Harris, E.; Sinha, B.; van Pinxteren, D.; Tilgner, A.; Fomba, K. W.; Schneider, J.; Roth, A.; Gnauk, T.; Fahlbusch, B.; Mertes, S.; Lee, T.; Collett, J.; Foley, S.; Borrmann, S.; Hoppe, P.; Herrmann, H. Enhanced Role of Transition Metal Ion Catalysis During In-Cloud Oxidation of SO2. *Science* **2013**, *340* (6133), 727−730.
(10) Kerminen, V.-M.; Teinilä, K.; Hillamo, R.; Pakkanen, T. Substitution of Chloride in Sea-Salt Particles by Inorganic and Organic Anions. *J. Aerosol Sci.* **1998**, *29* (8), 929−942.
(11) Kojima, T.; Buseck, P. R.; Iwasaka, Y.; Matsuki, A.; Trochkine, D. Sulfate-Coated Dust Particles in the Free Troposphere over Japan. *Atmos. Res.* **2006**, *82* (3−4), 698−708.
(12) Laskin, A.; Moffet, R. C.; Gilles, M. K.; Fast, J. D.; Zaveri, R. A.; Wang, B.; Nigge, P.; Shutthanandan, J. Tropospheric Chemistry of Internally Mixed Sea Salt and Organic Particles: Surprising Reactivity of NaCl with Weak Organic Acids. *J. Geophys. Res.* **2012**, *117* (D15), D15302.
(13) Reid, J. S.; Koppmann, R.; Eck, T. F.; Eleuterio, D. P. A Review of Biomass Burning Emissions Part II: Intensive Physical Properties of Biomass Burning Particles. *Atmos. Chem. Phys.* **2005**, *5* (3), 799−825.
(14) Zauscher, M. D.; Wang, Y.; Moore, M. J. K.; Gaston, C. J.; Prather, K. A. Air Quality Impact and Physicochemical Aging of Biomass Burning Aerosols during the 2007 San Diego Wildfires. *Environ. Sci. Technol.* **2013**, *47*, 7633−7643.
(15) Hinz, K.-P.; Trimborn, A.; Weingartner, E.; Henning, S.; Baltensperger, U.; Spengler, B. Aerosol Single Particle Composition at the Jungfraujoch. *J. Aerosol Sci.* **2005**, *36* (1), 123−145.
(16) Murphy, D. M.; Cziczo, D. J.; Froyd, K. D.; Hudson, P. K.; Matthew, B. M.; Middlebrook, A. M.; Peltier, R. E.; Sullivan, A.; Thomson, D. S.; Weber, R. J. Single-Particle Mass Spectrometry of Tropospheric Aerosol Particles. *J. Geophys. Res. Atmospheres* **2006**, *111* (D23), D007340.
(17) Sullivan, R. C.; Guazzotti, S. A.; Sodeman, D. A.; Prather, K. A. Direct Observations of the Atmospheric Processing of Asian Mineral Dust. *Atmos. Chem. Phys.* **2007**, *7* (5), 1213−1236.
(18) Ghorai, S.; Wang, B.; Tivanski, A.; Laskin, A. Hygroscopic Properties of Internally Mixed Particles Composed of NaCl and Water-Soluble Organic Acids. *Environ. Sci. Technol.* **2014**, *48* (4), 2234−2241.
(19) Wang, B.; O'Brien, R. E.; Kelly, S. T.; Shilling, J. E.; Moffet, R. C.; Gilles, M. K.; Laskin, A. Reactivity of Liquid and Semisolid Secondary Organic Carbon with Chloride and Nitrate in Atmospheric Aerosols. *J. Phys. Chem. A* **2015**, *119* (19), 4498−4508.
(20) Corr, C. A.; Ziemba, L. D.; Scheuer, E.; Anderson, B. E.; Beyersdorf, A. J.; Chen, G.; Crosbie, E.; Moore, R. H.; Shook, M.; Thornhill, K. L.; Winstead, E.; Lawson, R. P.; Barth, M. C.; Schroeder, J. R.; Blake, D. R.; Dibb, J. E. Observational Evidence for the Convective Transport of Dust over the Central United States. *J. Geophys. Res. Atmospheres* **2016**, *121* (3), 1306.
(21) Twohy, C. H.; Clement, C. F.; Gandrud, B. W.; Weinheimer, A. J.; Campos, T. L.; Baumgardner, D.; Brune, W. H.; Faloona, I.; Sachse, G. W.; Vay, S. A.; Tan, D. Deep Convection as a Source of New Particles in the Midlatitude Upper Troposphere. *J. Geophys. Res. Atmospheres* **2002**, *107* (D21), 4560.
(22) Cui, Z.; Carslaw, K. S. Enhanced Vertical Transport Efficiency of Aerosol in Convective Clouds due to Increases in Tropospheric Aerosol Abundance. *J. Geophys. Res.* **2006**, *111* (D15), D15212.
(23) Peng, C.; Chan, C. K. The Water Cycles of Water-Soluble Organic Salts of Atmospheric Importance. *Atmos. Environ.* **2001**, *35* (7), 1183−1192.
(24) Wu, Z. J.; Nowak, A.; Poulain, L.; Herrmann, H.; Wiedensohler, A. Hygroscopic Behavior of Atmospherically Relevant Water-Soluble Carboxylic Salts and Their Influence on the Water Uptake of Ammonium Sulfate. *Atmos. Chem. Phys.* **2011**, *11* (24), 12617−12626.
(25) Kissinger, J. A.; Buttke, L. G.; Vinokur, A. I.; Guzei, I. A.; Beyer, K. D. Solubilities and Glass Formation in Aqueous Solutions of the Sodium Salts of Malonic Acid With and Without Ammonium Sulfate. *J. Phys. Chem. A* **2016**, *120* (21), 3827−3834.
(26) Keller, H. L.; Kuppers, H. The Structure of the Monoclinic Low Temperature Modification of Ammonium Hydrogen Oxalate Hemihydrate. *Acta Crystallogr., Sect. A* **1978**, *34*, S104.
(27) Robertson, J. H. Ammonium Oxalate Monohydrate: Structure Refinement at 30 K. *Acta Crystallogr.* **1965**, *18* (3), 410−417.
(28) Chapuis, G.; Zalkin, A.; Templeton, D. H. Cyrstal Structure of Ammonium Hydrogen Malonate. *J. Chem. Phys.* **1975**, *62*, 4919−4922.
(29) Kloprogge, J. T.; Broekmans, M.; Duong, L. V.; Martens, W. N.; Hickey, L.; Frost, R. L. Low Temperature Synthesis and Characterisation of Lecontite, (NH4. *J. Mater. Sci.* **2006**, *41* (11), 3535−3539.
(30) Beyer, K. D.; Schroeder, J. R.; Kissinger, J. A. Temperature-Dependent Deliquescence Relative Humidities and Water Activities Using Humidity Controlled Thermogravimetric Analysis with Application to Malonic Acid. *J. Phys. Chem. A* **2014**, *118* (13), 2488−2497.
(31) Brooks, S. D.; Wise, M. E.; Cushing, M.; Tolbert, M. A. Deliquescence Behavior of Organic/Ammonium Sulfate Aerosol. *Geophys. Res. Lett.* **2002**, *29*, GL014733.
(32) Wise, M. E.; Surratt, J. D.; Curtis, D. B.; Shilling, J. E.; Tolbert, M. A. Hygroscopic Growth of Ammonium Sulfate/dicarboxylic Acids. *J. Geophys. Res.* **2003**, *108* (D20), D003775.
(33) Salcedo, D. Equilibrium Phase Diagrams of Aqueous Mixtures of Malonic Acid and Sulfate/ammonium Salts. *J. Phys. Chem. A* **2006**, *110*, 12158−12165.
(34) Parsons, M. T.; Knopf, D. A.; Bertram, A. K. Deliquescence and Crystallization of Ammonium Sulfate Particles Internally Mixed with Water-Soluble Organic Compounds. *J. Phys. Chem. A* **2004**, *108* (52), 11600−11608.
(35) Treuel, L.; Pederzani, S.; Zellner, R. Deliquescence Behaviour and Crystallisation of Ternary Ammonium Sulfate/dicarboxylic Acid/water Aerosols. *Phys. Chem. Chem. Phys.* **2009**, *11* (36), 7976−7984.
(36) Choi, M. Y.; Chan, C. K. The Effects of Organic Species on the Hygroscopic Behaviors of Inorganic Aerosols. *Environ. Sci. Technol.* **2002**, *36*, 2422−2428.
(37) Beyer, K. D.; Schroeder, J.; Palet, B. Solid/Liquid Phase Diagram of the Ammonium Sulfate/Malonic Acid/Water System. *J. Phys. Chem. A* **2010**, *114*, 4282−4288.
(38) Buttke, L. G.; Schueller, J. R.; Pearson, C. S.; Beyer, K. D. Solubility of the Sodium and Ammonium Salts of Oxalic Acid in Water with Ammonium Sulfate. *J. Phys. Chem. A* **2016**, *120* (32), 6424−6433.
(39) Linnow, K.; Zeunert, A.; Steiger, M. Investigation of Sodium Sulfate Phase Transitions in a Porous Material Using Humidity- and Temperature-Controlled X-Ray Diffraction. *Anal. Chem.* **2006**, *78* (13), 4683−4689.
(40) Beyer, K. D.; Schroeder, J. R.; Kissinger, J. A. Temperature-Dependent Deliquescence Relative Humidities and Water Activities Using Humidity Controlled Thermogravimetric Analysis with Application to Malonic Acid. *J. Phys. Chem. A* **2014**, *118* (13), 2488−2497.
(41) Apelblat, A.; Manzurola, E. Solubility of Oxalic, Malonic, Succinic, Adipic, Maleic, Malic, Citric, and Tartaric-Acids in Water from 278.15-K to 338.15-K. *J. Chem. Thermodyn.* **1987**, *19*, 317−320.
(42) Braban, C. F. *Laboratory Studies of Model Tropospheric Aerosol Phase Transitions*; University of Toronto: Toronto, 2004.

DOI: 10.1021/acs.jpca.6b08725
J. Phys. Chem. A 2016, 120, 9948−9957